sustainability

Article

Assessing the Net Primary Productivity Dynamics of the Desert Steppe in Northern China during the Past 20 Years and Its Response to Climate Change

Bo Yang *, Xiaoshuang Li, Yaqi Xian, Yalin Chai, Min Li, Kaidie Yang and Xiaorui Qiu

College of Tourism, Northwest Normal University, Lanzhou 730070, China; lixiaoshuang0723@126.com (X.L.); xianyaqi8793@163.com (Y.X.); sarin@sina.com (Y.C.); liminee1206@163.com (M.L.); h17339832649@163.com (K.Y.); qxrui2418@126.com (X.Q.)

* Correspondence: yangbo907@126.com

Abstract: The net primary productivity (*NPP*) dynamics in arid and semi-arid ecosystems are critical for regional carbon management. Our study applied a light-utilization-efficiency model (CASA: Carnegie–Ames–Stanford Approach) to evaluate the vegetation *NPP* dynamics of a desert steppe in northern China over the past 20 years, and its response to climate change. Our results show that the annual average *NPP* of the desert steppe was 132 g C m^{-2} y^{-1}, of which the grass- and shrub-dominated biome values were 142 and 91 g C m^{-2} y^{-1}, respectively. The average change rate of *NPP* was 1.13 g C m^{-2} y^{-1}, and in the grassland biome 1.31 g C m^{-2} y^{-1}, a value which was significantly higher than that in shrubland, at 0.84 g C m^{-2} y^{-1}. The precipitation and temperature at different time scales in the desert steppe showed a slow upward trend, and the degree of aridity tended to weaken. The correlation analysis shows that *NPP* changes were significantly positively and negatively correlated with precipitation and temperature, respectively. In terms of temperature, 43% of the area was significantly correlated during the growing season, which decreased to 12% on the annual scale. In 31% of the changed areas, the average *NPP* was 148.1 g C m^{-2} y^{-1}, which was higher than the remaining significant areas. This suggests that higher *NPP* levels help to attenuate the negative effects of high temperature during the growing season on plant productivity in the desert steppe. This improves the understanding of the carbon cycle mechanism of arid and semi-arid ecosystems, which is beneficial to improving sustainable grassland development strategies.

Keywords: *NPP* simulation; CASA model; semi-arid ecosystems; desert steppe; climate change

check for updates

Citation: Yang, B.; Li, X.; Xian, Y.; Chai, Y.; Li, M.; Yang, K.; Qiu, X. Assessing the Net Primary Productivity Dynamics of the Desert Steppe in Northern China during the Past 20 Years and Its Response to Climate Change. *Sustainability* **2022**, *14*, 5581. https://doi.org/10.3390/su14095581

Academic Editors: Juejie Yang, Shikui Dong, Lin Liu and Fei Li

Received: 19 March 2022
Accepted: 4 May 2022
Published: 6 May 2022

Publisher's Note: MDPI stays neutral with regard to jurisdictional claims in published maps and institutional affiliations.

Copyright: © 2022 by the authors. Licensee MDPI, Basel, Switzerland. This article is an open access article distributed under the terms and conditions of the Creative Commons Attribution (CC BY) license (https://creativecommons.org/licenses/by/4.0/).

1. Introduction

The vegetation net primary productivity (*NPP*) is an important indicator when quantifying ecosystem carbon cycling, services, and sustainability [1,2]. In terrestrial ecosystems, grassland ecosystems play an important role in global carbon dynamics, climate change, and food security [3]. Changes in vegetation *NPP* may alter soil erosion and mineralization and carbon cycling processes in grassland ecosystems by loss of plant coverage [4], thereby increasing the risks of soil carbon loss and soil degradation [5]. Climate change plays a critical role in the driving mechanism of natural grassland productivity change [6,7]. Vegetation productivity has often been clearly affected by climate change and frequent drought events in grasslands [8]. In addition, climate heterogeneity will cause vegetation to form a unique community structure and develop efficient light utilization strategies [9]. The spatial distribution of grassland *NPP* in turn shows corresponding heterogeneity characteristics. Therefore, the response of grassland productivity to climate change at different time scales and in different vegetation communities needs to be further clarified.

The Inner Mongolian plateau steppe is a major component of the Eurasian steppe, and its productivity is highly sensitive to climate change. The Inner Mongolian Plateau is controlled by the strong Mongolian high pressure in winter, and most areas are affected by the East Asian monsoon in summer [10,11]. This makes the vegetation productivity of the temperate grasslands here one of the most sensitive to climate change in the world. Previous studies have shown that temperature and precipitation have been rising and falling in Mongolia's temperate grasslands, respectively [12,13]. In detail, climate warming could inhibit the productivity of Mongolian grasslands [14]. Changes in interannual precipitation could drive changes in net primary productivity [15]. However, the time scale of these analyses of the impact of climatic factors on *NPP* is usually of years or growing seasons. Therefore, the impact of climate variables at different time scales on *NPP* needs further research.

In arid and semi-arid ecosystems, frequent drought events may lead to shrub invasion in grassland ecosystems [16]. Climate change may affect *NPP* by altering the vegetation structure and species composition of temperate grasslands. This phenomenon may cause the original grass-dominated community structure to transition into a shrub-dominated community. The shrub invasion may change the original light utilization efficiency and water-use mechanisms of the communities in temperate grasslands [17], thereby affecting the net primary productivity of grassland vegetation [18]. Temperature and water conditions could regulate the *NPP* of vegetation by affecting the photosynthetic capacity of plants [19]. In the remote-sensing model, the regulation of these *NPP*s is achieved by correcting the maximum light utilization efficiency [19]. In conclusion, changes in community structure will change the value of maximum light utilization efficiency, which in turn will change the estimate of *NPP*. Therefore, it is necessary to distinguish community types in the estimation of *NPP* and the observation of its responses to climate change in temperate grasslands.

A light utilization efficiency (LUE) scheme, the Carnegie–Ames–Stanford Approach (CASA), has been widely used to estimate the *NPP* of different vegetation types in terrestrial ecosystems. The CASA takes into account the relationship between productivity and photosynthetically active radiation and environmental variables in estimating *NPP* [20–22]. During simulations using previous versions of the CASA model, the accuracy of the vegetation-type map has been relatively poor, the maximum light utilization efficiency of vegetation has been low, and the soil moisture model parameters have been difficult to measure [23]. These factors increase uncertainty in *NPP* estimates. Zhu improved the uncertainty of *NPP* estimates from the original CASA model [19,24]. In addition, the cold–temperate desert steppe is located in the transition zone between desert and steppe in the central part of the Inner Mongolia Autonomous Region. This region consists of grass-dominated and shrub-dominated biomes. It is an important part of the temperate steppe and an important livestock production base for northern China, accounting for about 34.7% of its grassland [25]. Therefore, we applied an improved CASA model to estimate *NPP* at different time scales and in different communities of the desert steppe.

We hypothesized that the response of *NPP* to climate change at different time scales would differ by biome type. The objectives were to (1) simulate and estimate *NPP* in different biomes in the desert steppe from 2000 to 2017; (2) assess changes in *NPP* over temporal and spatial ranges; and (3) explore the response patterns of *NPP* in different biomes to climatic parameters at different time scales.

2. Materials and Methods

2.1. Study Area

Our study area is located in the transition zone between desert and steppe in northern China, which is a cold–temperate desert steppe in the southern part of the Inner Mongolian Plateau (40°50′ N to 45°20′ N and 106°10′ E to 114°50′ E). Our study area was mainly distributed over the following counties in the Inner Mongolia Autonomous Region of China: Sunitezuo, Suniteyou, Erlianhaote, Siziwang, Daerhanmaomingan, Wulatezhong, and Wulatehou from east to west (Figure 1). The desert steppe has poor climate conditions. The population density is less than 10 people per square kilometer, but the town is highly concentrated. This environmental condition provides a relatively independent platform for our observations. In addition, the desert steppe is located at the edge of the area influenced by the East Asian summer monsoon and is therefore affected by the alternation between temperate continental and monsoon climates. Our statistics show that from 2000 to 2017, the mean annual temperature ranged from 3 °C in the northeast to 8 °C in the southwest, and the mean annual precipitation ranged from 145 mm in the west to 320 mm in the south. Precipitation mainly occurs from May to September, accounting for 85% of the annual precipitation. The growing season in the region begins in April and ends in October, with precipitation reaching its maximum in August [26]. The grassland plant community consists of grass-dominated and shrub-dominated biomes, and the dominant plant species include *Stipa klemenzii*, *Stipa breviflora*, *Stipa glareosa*, *Salsola collina*, *Cleistogenes songorica*, and *Artemisia frigida*. The soils in our study area are dominated by *Kastanozems* and *Calcisols* from east to west (Figure 1).

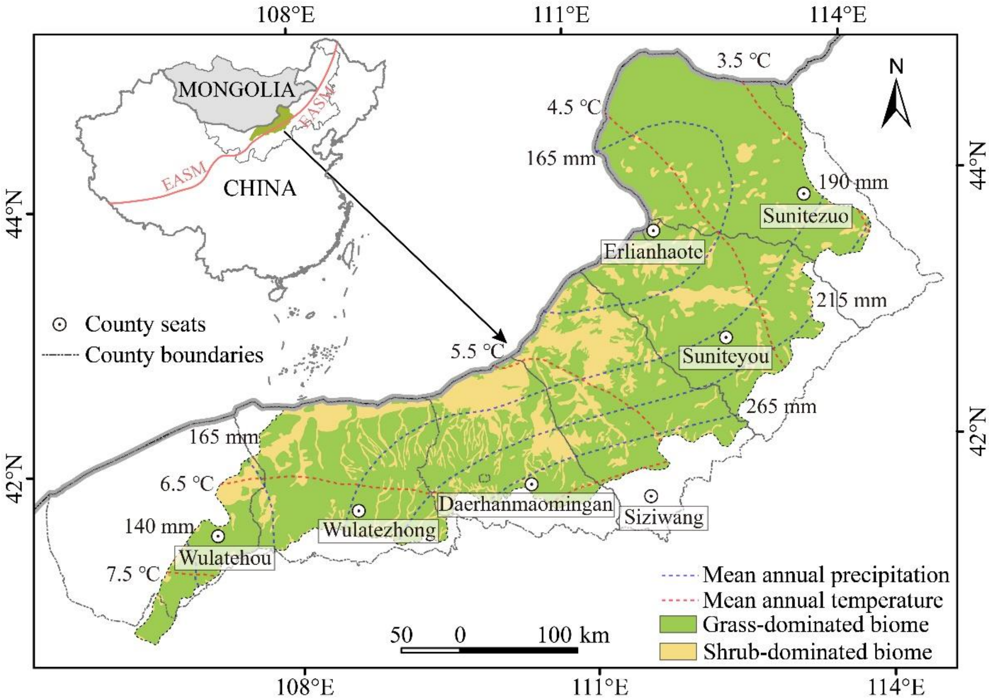

Figure 1. Spatial distribution map of biomes dominated by grass and shrubs in the temperate desert steppe in the Inner Mongolia Autonomous Region. Isolines are for the mean annual precipitation and mean annual temperature based on data from 2000 to 2017. The inset map shows the northern limit of the East Asian Summer Monsoon (EASM).

2.2. Simulation of *NPP*

According to the suitability of the CASA model, we applied the improved CASA to estimate *NPP* [24]. The estimated *NPP* in the model is represented by the Absorbed Photosynthetically Active Radiation (*APAR*) and the actual light utilization efficiency (ε). Therefore, ε can be described by:

$$NPP\ (x,\ t) = APAR\ (x,\ t)\ \times\ \varepsilon\ (x,\ t) \tag{1}$$

where $\varepsilon(x, t)$ represents the actual light utilization efficiency of pixel x in month t (g C/MJ); $APAR(x,\ t)$ represents the light and effective radiation absorbed by pixel x in month t (MJ/m^2/month).

2.2.1. Estimation of *APAR*

We used remote-sensing data to estimate the fraction of photosynthetically active radiation (*PAR*) absorbed by plant leaves (*APAR*). This process is based on the reflection characteristics of vegetation in the infrared and near-infrared bands. Photosynthetically active radiation (*PAR*, 0.4–0.7 um) is the driving force for plant photosynthesis, the capture and utilization of which by plants is a necessary for the origin, evolution, and persistence of the biosphere. The photosynthetically active radiation absorbed by plants depends on the characteristics of the vegetation itself and the total amount of solar radiation. Therefore, *APAR* can be described by:

$$APAR\ (x,\ t) = SOL\ (x,\ t)\ \times\ FPAR\ (x,\ t)\ \times\ 0.5 \tag{2}$$

where $SOL(x, t)$ represents the total solar radiation of pixel x in month t (MJ/m^2/month); $FPAR(x, t)$ is the absorption ratio (unitless) of the vegetation layer to the incident light and effective radiation; the constant 0.5 refers to the ratio of the effective solar radiation that can be used by vegetation to the total solar radiation (wavelength is 0.38–0.71 um).

There is a linear relationship between *FPAR* and *NDVI* within a certain range [27]. This relationship can be determined based on the maximum and minimum *NDVI* values for a certain vegetation type.

$$FPAR\ (x,\ t) = \frac{(NDVI\ (x,\ t) - NDVI_{i,\ min}) \times\ (FPAR_{max} - FPAR_{min})}{(NDVI_{i,\ max} - NDVI_{i,min})} + FPAR_{min} \tag{3}$$

where $NDVI_{i,max}$ and $NDVI_{i,min}$ are the maximum value and minimum value of *NDVI* that can appear for the *i*-th vegetation type during the study period, respectively.

There is a linear relationship between *FPAR* and the ratio vegetation index (*SR*), which can be described by:

$$FPAR\ (x,\ t) = \frac{(SR\ (x,\ t) - SR_{i,\ min}) \times\ (FPAR_{max} - FPAR_{min})}{(SR_{i,\ max} - SR_{i,min})} + FPAR_{min} \tag{4}$$

where $FPAR_{max}$ and $FPAR_{min}$ are 0.95 and 0.001, respectively, and are independent of the vegetation type. *SR* was determined by the following equation, where $SR_{i,max}$ and $SR_{i,min}$ correspond to the 95th and 5% lower percentiles of *NDVI* for the first vegetation type, respectively.

$$SR\ (x,\ t) = [\frac{1 +\ NDVI\ (x,\ t)}{1 -\ NDVI\ (x,\ t)}] \tag{5}$$

The *FPAR* estimated by *NDVI* is higher than the measured value, and the *FPAR* estimated by *SR* is lower than the measured value. Therefore, we take the mean value as an estimate of *FPAR* to minimize the error.

$$FPAR\ (x,\ t) = \alpha FPAR_{NDVI} + (1-\alpha)FPAR_{SR} \tag{6}$$

where α is the adjustment coefficient of the two methods, and we determine it to be 0.5 (the average of the two).

2.2.2. Estimation of Actual Light Utilization Efficiency

Vegetation has a maximum light utilization efficiency (ε_{max}) only under ideal conditions, while ε_{max} in practical conditions will be affected by moisture and temperature. It can be described by:

$$\varepsilon(x,\ t) = T_{\varepsilon 1}\ (x,\ t) \times T_{\varepsilon 2}\ (x,\ t) \times W_{\varepsilon}\ (x,\ t) \times \varepsilon_{max} \tag{7}$$

where $\varepsilon(x, t)$ is the actual utilization rate of light energy, $T_{\varepsilon 1}(x, t)$ and $T_{\varepsilon 2}(x, t)$ represent the stressing effect of low temperatures and high temperatures on the utilization rate of light energy (unitless), respectively, and $W_{\varepsilon}(x, t)$ is the water-stress influence coefficient (unitless).

$T_{\varepsilon 1}(x, t)$ reflects the limitation of photosynthesis by intrinsic plant biochemistry at low temperatures and high temperatures and reduces net primary productivity.

$$T_{\varepsilon 1}\ (x,\ t) = 0.8 + 0.02\ \times\ T_{opt}(x)\ - 0.0005 \times [T_{opt}(x)]^2 \tag{8}$$

where $T_{opt}(x)$ represents the optimum temperature. It is the monthly average temperature (°C) when the *NDVI* value reaches the highest value in a certain region within a year. When the average temperature of a certain month is less than or equal to −10 °C, $T_{\varepsilon 1}(x, t)$ is 0.

When the ambient temperature changes from the optimum temperature $T_{opt}(x)$ to a higher or lower temperature, the trend by which plant light utilization gradually decreases is $T_{\varepsilon 2}(x, t)$.

$$T_{\varepsilon 2}\ (x,\ t) = 1.184/\left\{1 + exp\left[0.2 \times \left(T_{opt}(x)\ - 10 - T(x,\ t)\right)\right]\right\} \\ \times 1/\left\{1 + exp\left[0.3 \times \left(-T_{opt}(x)\ - 10 + T(x,\ t)\right)\right]\right\} \tag{9}$$

where $T(x, t)$ is the average temperature (°C) of a certain month.

The influence coefficient of water stress, $W_\varepsilon(x, t)$, reflects the effect of the effective water condition that plants can use on light utilization. As the available moisture increases in the environment, $W_\varepsilon(x, t)$ increases gradually. Its value ranges from 0.5 (in extremely dry conditions) to 1 (in very wet conditions).

$$W_\varepsilon\ (x,\ t) = 0.5 + 0.5\ \times\ E\ (x,\ t)\ /\ E_p\ (x,\ t) \tag{10}$$

where $E(x, t)$ is the regional actual evapotranspiration (mm) and $E_p(x, t)$ is the regional potential evapotranspiration (mm).

Monthly maximum utilization efficiency, ε_{max}, varies with vegetation types. The global maximum light utilization efficiency used in the initial version of the CASA model shows a lower *NPP* estimate for China. Zhu, Pan, He, Wang, Mou and Liu [23] calculated the *APAR* of the pixel, considering the influence of temperature and water stress factors. They simulated the ε_{max} of each vegetation type by comparing the measured *NPP* values in the same time period, following the principle of minimum error. The results show that the ε_{max} of temperate grassland and shrubland is 0.542 and 0.429 g C/MJ, respectively, which is well-verified in practical applications [19]. Therefore, this ε_{max} value is also used in our study.

2.3. Estimation of SPEI

The FAO-56 Penman–Monteith equation was used to calculate the standardized precipitation–evapotranspiration index (*SPEI*) and was used to represent potential evapotranspiration. The important climatological and ecological index, *SPEI*, can be used to explore the extent of drought and its potential impact on ecosystem cycle processes [28]. The procedure for calculating this index was described in detail in a study by Beguería et al. [29]. The value of *SPEI* can reflect previous states of water balance or abnormality in different periods [30]. We applied *SPEI* to reflect changes in the water status of the study area on seasonal and annual scales, as well as changes over the entire study period.

2.4. Data Description and Statistics

We obtained the MODIS MOD13Q1 Terra vegetation *NDVI* from the NASA Reverb website (https://earthdata.nasa.gov/, accessed on 18 March 2022) from 2000 to 2017, which we used for the *NPP* simulation. The MOD13Q1 data had a spatial resolution of 250 m and a temporal resolution of 16 days. We used the quality assurance band and a composite day band as ancillary data before the *NPP* simulation. Cloud contamination was determined when a point in the time series had a vegetation index usefulness index greater than 8. In such cases, we used linear interpolation of adjacent points instead. There were extremely noisy points, with a random *NDVI* increase or decrease by more than 0.4, on 16 days, and these were also rejected and replaced by linearly interpolated values using adjacent points. We then linearly interpolated the unevenly spaced *NDVI* time series using composite daily bands. *NDVI* time-series preprocessing was reconstructed by harmonic analysis of time series (HANTS) filtering [31].

Land use data from the Inner Mongolia Autonomous Region in 2015 were collected from the Resource and Environmental Science and Data Center of the Institute of Geographical Sciences and Natural Resources Research, Chinese Academy of Sciences (https://www.resdc.cn, accessed on 18 March 2022). The vegetation types in Figure 1 were extracted from a map of vegetation types in China with a scale of 1:1,000,000 [32]. The meteorological data sources in the study area from 2000 to 2017 were obtained from the China Meteorological Data Sharing Service System (http://data.cma.cn, accessed on 18 March 2022). Among them, the monthly average solar radiation was obtained from 99 national standard meteorological stations in China, and the monthly average temperature and monthly total precipitation were recorded by 39 national standard meteorological stations in the Inner Mongolia Autonomous Region. Furthermore, data were statistically analyzed using one-way analysis of variance (ANOVA) followed by Fisher's LSD test ($p < 0.05$). To assess the association between *NPP* and climatic factors of precipitation, temperature, and *SPEI* at <0.05 significance (p) level, the Pearson correlation (r) analysis was used.

3. Results

3.1. Temporal and Spatial Variation of NPP

The annual average *NPP* in the desert steppe from 2000 to 2017 was 131.93 g C m^{-2} y^{-1} (Figure 2a). The annual average *NPP* of grass- and shrub-dominated biomes were 141.8 and 90.6 g C m^{-2} y^{-1}, respectively. This is consistent with the original reference for improved CASA [33]. The highest *NPP* value in the study area appeared in the southeast, with an average value higher than 220 g C m^{-2} y^{-1}, but the area accounted for only 2.9%. The lower *NPP* values appear in the middle and western regions, and 60% of the study areas have *NPP* values below 140 g C m^{-2} y^{-1}. Over the past two decades, the change in *NPP* showed obvious spatial heterogeneity (Figure 2b). The average annual change rate of *NPP* was 1.13 g C m^{-2} y^{-1}, and 72.4% of the study area had a positive *NPP* change rate. There was a trend of *NPP* decline in the central and eastern areas (from –1 to –2 g C m^{-2} y^{-1}), but only in 1.6% of the total area. The areas with significant changes in *NPP* accounted for 5.5% of the total area ($p < 0.05$), of which 98% were significantly increased. Biome comparison showed that the average increase rates of grassland and shrubland were 1.31 and 0.84 g C m^{-2} y^{-1}, respectively, and the former was significantly higher than the latter ($p < 0.05$).

3.2. Changes in Climate Variables

The average annual precipitation in the desert steppe was 186.7 mm, with an annual increase of 0.41 mm (Figure 3). The average precipitation in the growing and non-growing seasons was 173.8 and 12.9 mm, respectively. The average precipitation outside of the growing season accounted for 7% of the average annual total precipitation, with an average annual increase rate of 2.0%, 0.27 mm y^{-1}. The annual increase rate was significantly higher than during the growing season, which was 0.12% (i.e., 0.23 mm y^{-1}). In the grassland biome, the precipitation during the growing season and outside the growing season was 175.2 and 12.4 mm, respectively. In the shrub-dominated biome area, precipitation during the growing season and outside of the growing season was 166.9 and 11.8 mm, respectively. Furthermore, the rate of increase in precipitation in the grassland biome was higher than that in shrubland, especially in the growing season.

The mean annual temperature outside of the growing season increased by about 1.0 °C during the past two decades in the study area, which was higher than that during the growing season (+0.38 °C) and the annual average temperature (+0.59 °C). The average temperature in the grassland biome area was 15.5 °C and −9.2 °C in the growing and outside of the growing seasons, respectively (Figure 4). For the shrubland, the average temperature during the growing season and outside the growing season was 15.7 and −8.7 °C, respectively. The temperature change rates of grass- and shrub-dominated biomes at different temporal scales were consistent.

The minimum and maximum *SPEI* values of the desert steppe at the annual scale were −2.13 and 1.55, respectively (Figure 5). The average annual minimum and maximum values of *SPEI* during the growing season were −1.98 and 1.61, respectively. There was a marked alternation between wet and dry years during the over past two decades.

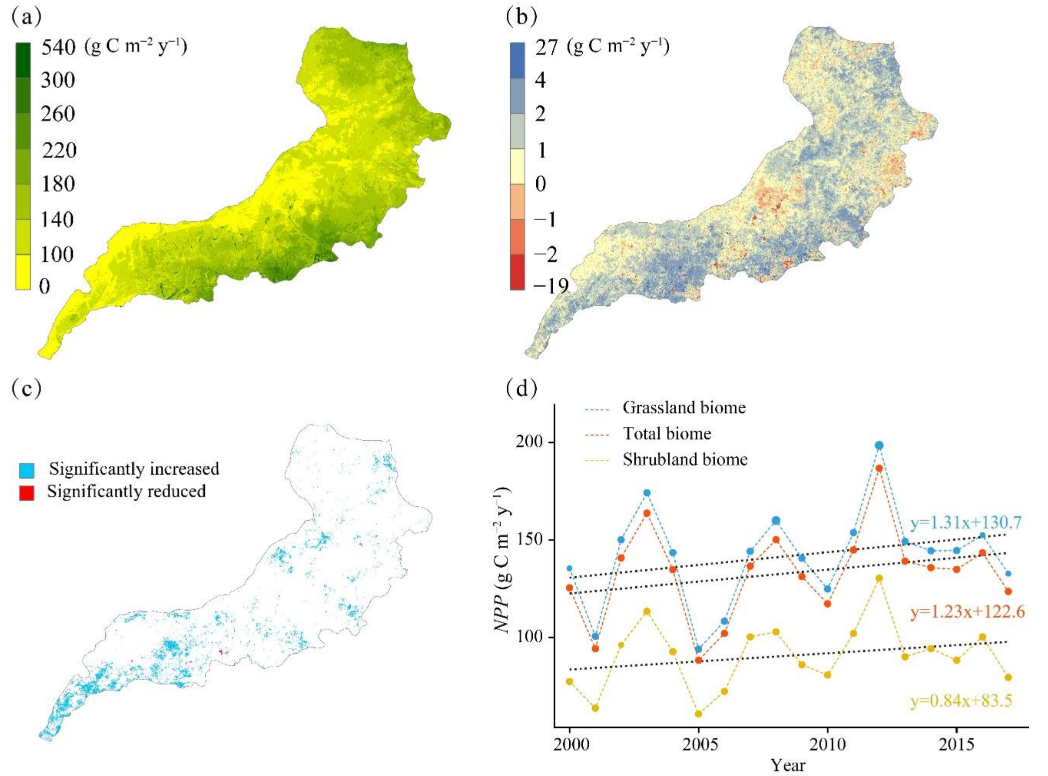

Figure 2. Spatial distribution and trend statistics of *NPP* in the desert steppe from 2000 to 2017. (**a**) Spatial patterns of the average *NPP*. (**b**) The change rate of *NPP*. (**c**) Significance statistics for the change rate ($p < 0.05$). (**d**) *NPP* trends in two biomes and total area of the desert steppe ($p > 0.05$ for statistical results).

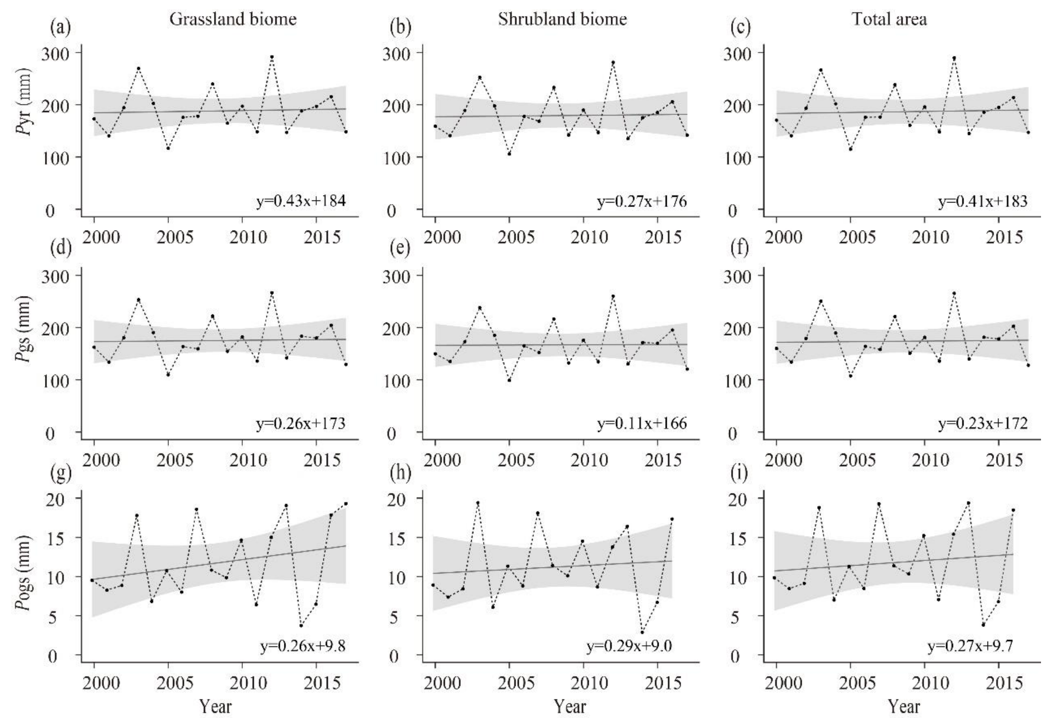

Figure 3. The precipitation changes of the different temporal scales (grassland biome, shrubland biome, and total area) from 2000 to 2017 ($p > 0.05$ for statistical results). P_{yr}, total annual precipitation (**a**–**c**); P_{gs}, precipitation during the growing season (**d**–**f**); P_{ogs}, precipitation outside the growing season (**g**–**i**). The shadow represents the 95% confidence interval of the fitted line.

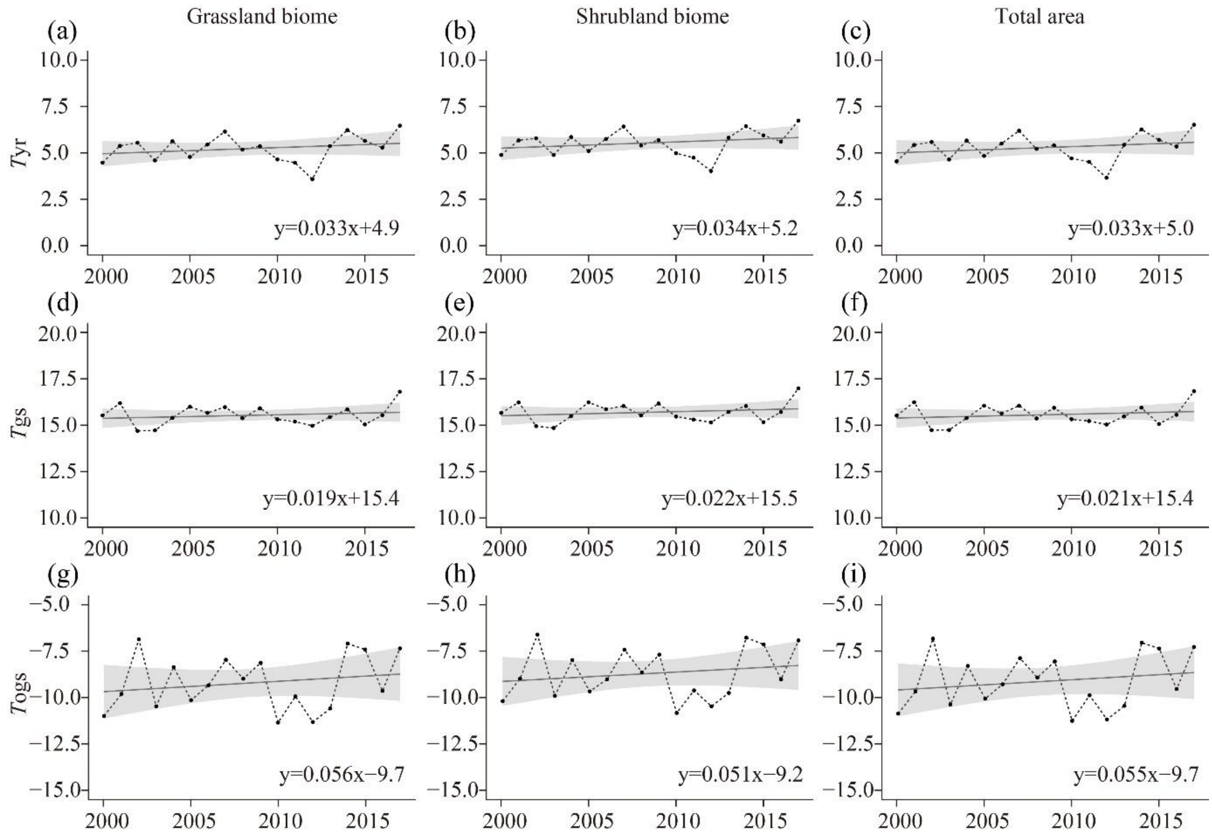

Figure 4. The temperature changes of the different temporal scales (grassland biome, shrubland biome, and total area) from 2000 to 2017 ($p > 0.05$ for statistical results). T_{yr}, average annual temperature (**a**–**c**); T_{gs}, daily average temperature during the growing season (**d**–**f**); T_{ogs}, daily average temperature outside the growing season (**g**–**i**). The shadow represents the 95% confidence interval of the fitted line.

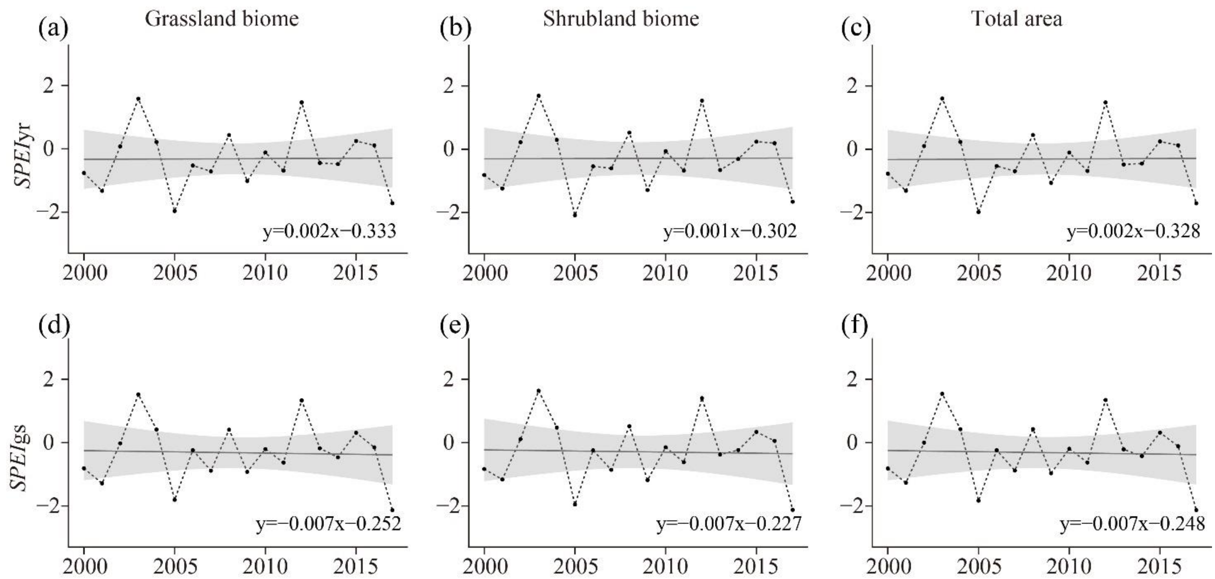

Figure 5. The *SPEI* of the different temporal scales (grassland biome, shrubland biome, and total area) from 2000 to 2017 ($p > 0.05$ for statistical results). $SPEI_{yr}$, annual average standardized precipitation–evapotranspiration index (*SPEI*) (**a**–**c**); $SPEI_{gs}$, the *SPEI* during the growing season (**d**–**f**). The shadow represents the 95% confidence interval of the fitted line.

3.3. Correlations between NPP Changes and Climate Variables

We explored the potential driving mechanisms of *NPP* changes in different biomes by analyzing the correlations between *NPP* and major climate driving variables (Figure 6). Overall, the *NPP* responses of grass- and shrub-dominated biomes to climate change were consistent. There was a significant positive correlation between precipitation and *NPP* change. Precipitation during the growing season had a particular and significant promoting effect on *NPP* change. The temperature was negatively correlated with *NPP* change. This shows that the temperature increase has an inhibitory effect on the increase in *NPP*, especially in the growing season. There was a significant positive correlation between the *SPEI* value and the change in *NPP*. The shows that the *NPP* variation of the desert steppe was highly dependent on water conditions.

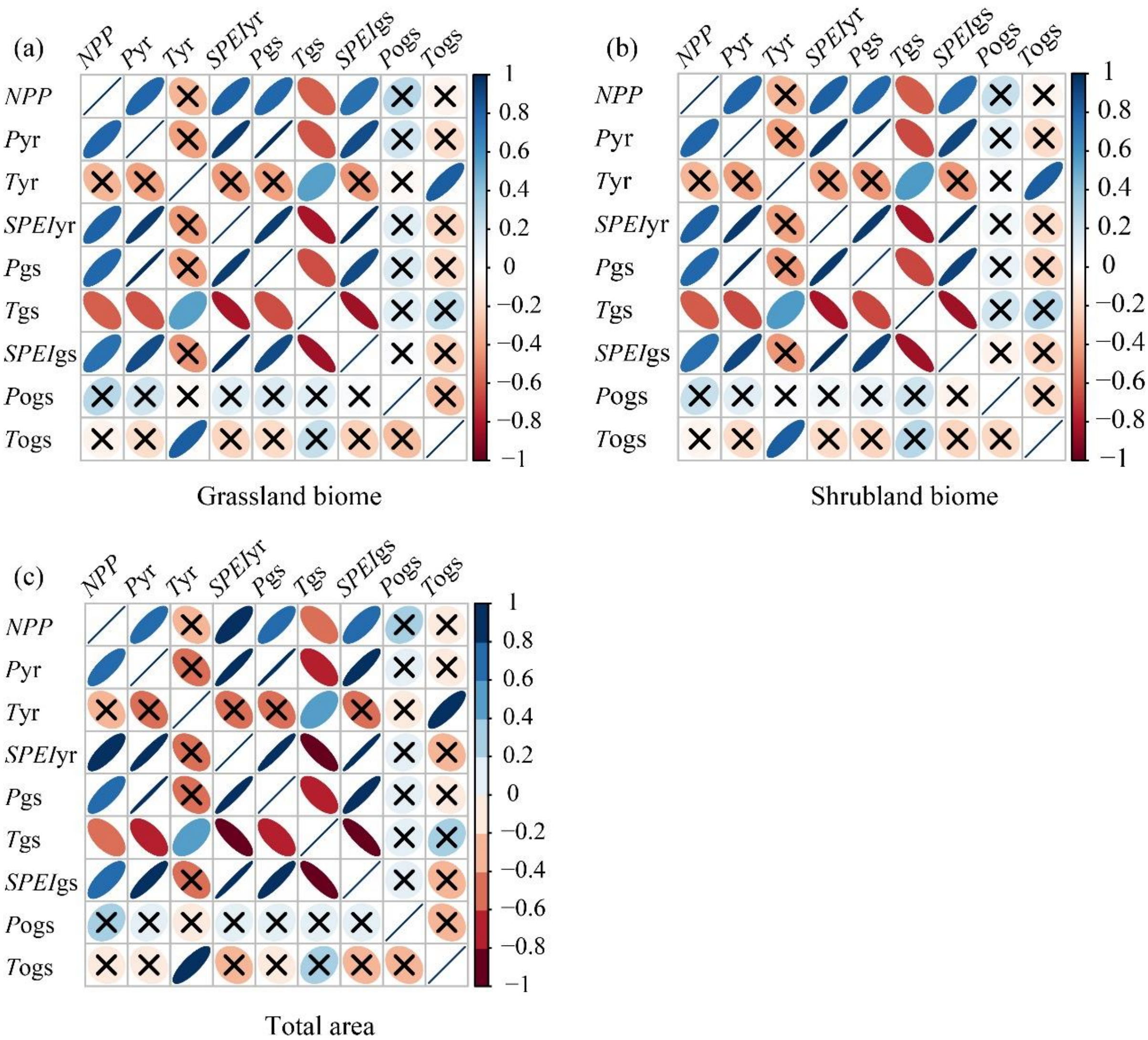

Figure 6. Summary of correlations between the *NPP* and climate variables (Pearson's *r*) at different time scales ((**a**), grassland biome; (**b**), shrubland biome; (**c**), and total area) from 2000 to 2017. *NPP*—net primary productivity; P_{yr}—total annual precipitation; T_{yr}—average annual temperature; $SPEI_{yr}$—annual average standardized precipitation—evapotranspiration index (*SPEI*); P_{gs}—precipitation during the growing season; T_{gs}—daily average temperature during the growing season; $SPEI_{gs}$—the average *SPEI* during the growing season. P_{ogs}—precipitation outside the growing season; T_{ogs}—daily average temperature outside the growing season. The cross showed no statistically significant correlation, and the width and orientation of the ellipse represent the correlation coefficient values and positive or negative correlation.

3.4. Impact of Climate Change on NPP Dynamics

In arid and semi-arid regions, changes in annual precipitation often have a significant impact on *NPP*. In our study, *NPP* was significantly positively correlated with changes in annual precipitation (P_{yr}) and growing season precipitation (P_{gs}), and the area proportions with significant correlation were 91% and 89%, respectively (Figure 7). There was a significant positive correlation between *NPP* and precipitation outside of the growing season (P_{ogs}) in the eastern part of the study area (1.7% of the total area). This indicates that the increase in *NPP* in the desert steppe may benefit from the increase in precipitation outside of the growing season.

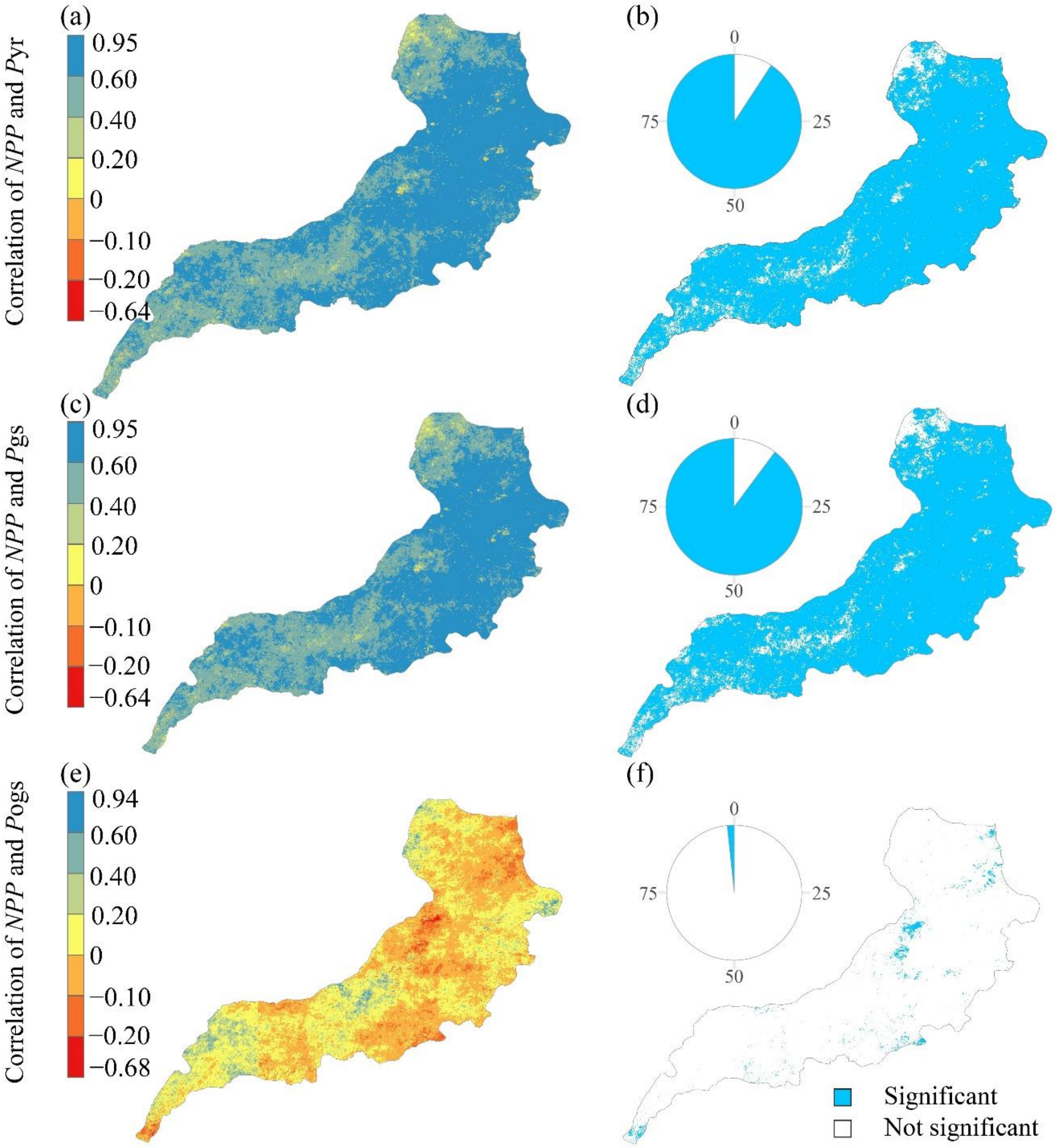

Figure 7. The spatial distribution of the correlation between *NPP* and temperature (Pearson's *r*) at different temporal scales ((**a**,**b**), annual; (**c**,**d**), growing season; and (**e**,**f**), outside the growing season). Blue areas in the inset map indicate statistically significant correlations, white areas indicate no statistical significance. P_{yr}—total annual precipitation; P_{gs}—precipitation during the growing season; P_{ogs}—precipitation outside the growing season.

Based on the correlation analysis of temperature and *NPP*, there was a significant negative correlation of *NPP* changes with T_{yr}, T_{gs}, and T_{ogs}, respectively, and the area proportions were 12%, 43%, and 0.4%. It was shown that temperature increases at different time scales had negative effects on *NPP* (Figure 8). In the eastern part of the study area, with higher latitude, there was a positive correlation between *NPP* and T_{ogs}. This indicates that the temperature increases outside of the growing season may promote *NPP*. In comparison, it was found that the temperature rises in the growing season had a significant negative effect on *NPP* in 43% of the area. This was a significantly larger area than the 12% seen for significant responses to annual temperature changes.

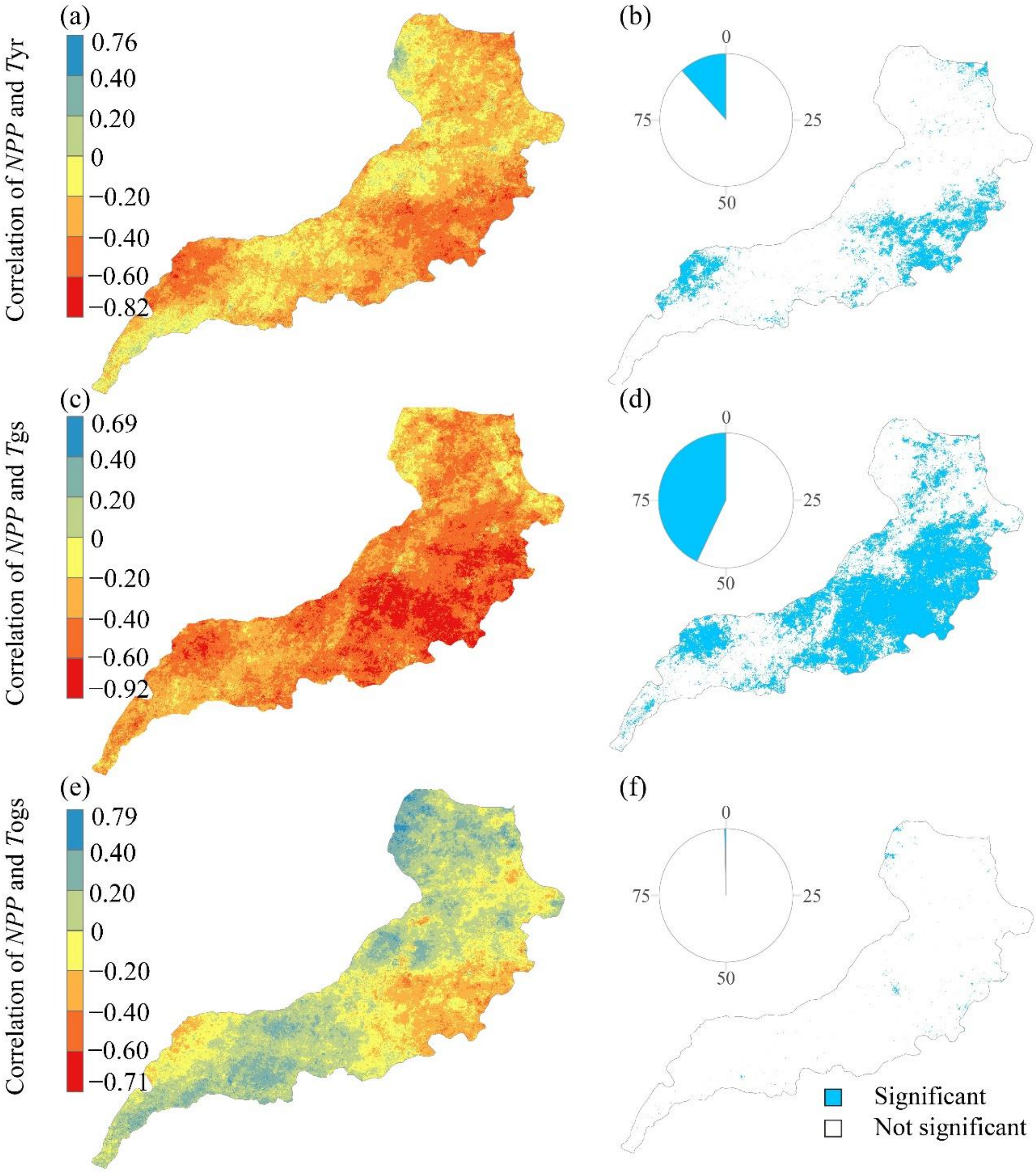

Figure 8. The spatial distribution of the correlation between *NPP* and temperature (Pearson's *r*) at different temporal scales ((**a**,**b**), annual; (**c**,**d**), growing season; and (**e**,**f**), outside the growing season). Blue areas in the inset map indicate statistically significant correlations, white areas indicate no statistical significance. T_{yr}—average annual temperature; T_{gs}—daily average temperature during the growing season; T_{ogs}—daily average temperature outside the growing season.

SPEI could be used to determine the occurrence, duration and intensity of droughts. In our study, more than 80% of the area represented a significant positive correlation between *NPP* and $SPEI_{yr}$ and $SPEI_{gs}$ (Figure 9). The annual *NPP* changes represented a significant positive correlation with $SPEI_{yr}$ and $SPEI_{gs}$ in 90% and 82% of the study area, respectively. The average values of both $SPEI_{yr}$ and $SPEI_{gs}$ were less than 0, which also proved that *NPP* in the study area was significantly affected by wet and dry conditions.

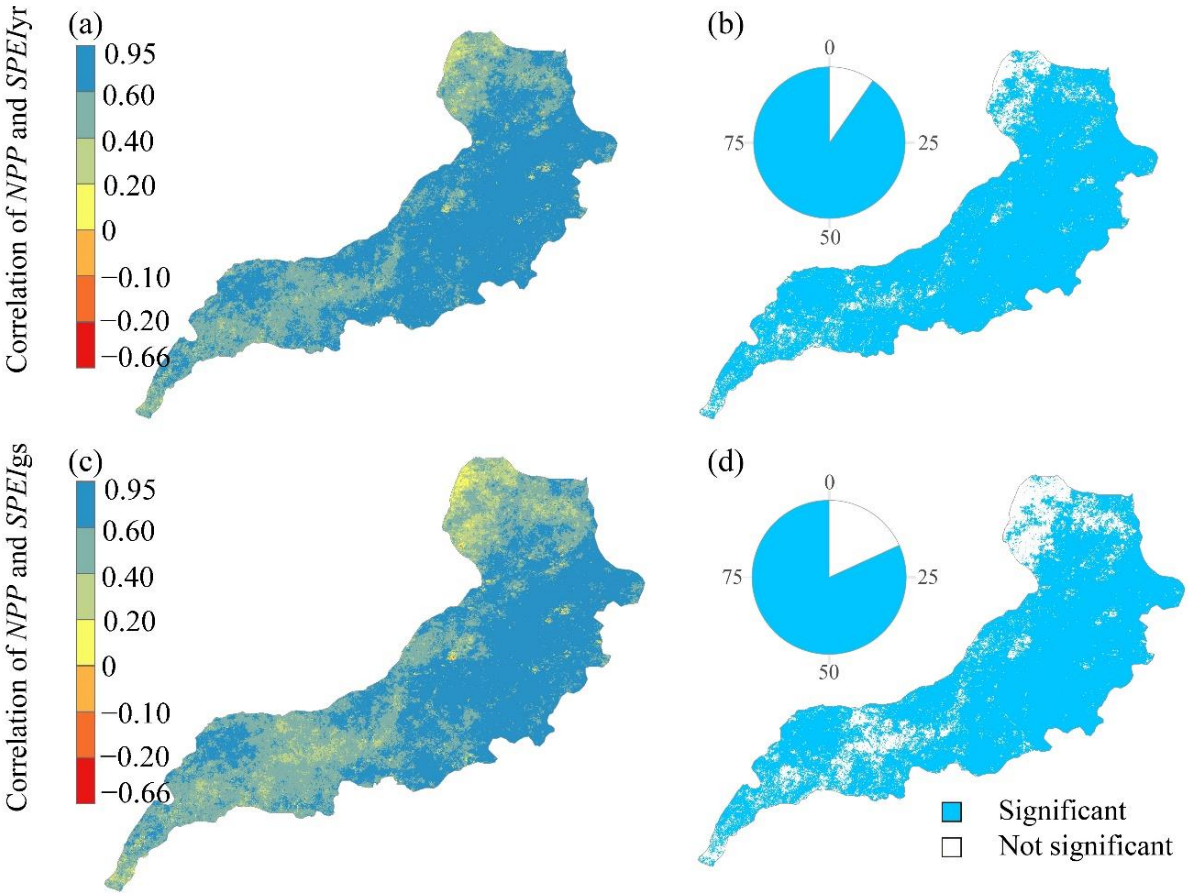

Figure 9. Spatial pattern of the correlation (Pearson's *r*) between *NPP* and the standardized precipitation—evapotranspiration index (Pearson's *r*) at different temporal scales ((**a**,**b**), annual; (**c**,**d**), growing season). In the inset map, blue areas show statistically significant correlations and white areas show no statistically significant correlation. $SPEI_{yr}$—annual mean standardized precipitation—evapotranspiration index (*SPEI*); $SPEI_{gs}$—the *SPEI* during the growing season.

4. Discussion

4.1. NPP Magnitude and Distribution

Accurately quantifying vegetation *NPP* of different community types is an important condition for understanding the ecosystem carbon cycle and predicting the impact of climate change [34,35]. The sensitivity of desert steppe *NPP* to environmental changes determines the importance of its *NPP* dynamics in terms of the regional and terrestrial ecosystem carbon budget. The annual average *NPP* of the study region over the past two decades was 131.93 g C m^{-2} y^{-1}. Compared with the grassland types adjacent to the desert steppe, the annual average *NPP* of the temperate typical steppe and meadow steppe were usually greater than 150 and 250 g C m^{-2} y^{-1}, respectively [36]. The annual average *NPP* of grass- and shrub-dominated biomes were 141.8 and 90.6 g C m^{-2} y^{-1}, respectively. The value of the grassland biome was higher than that of the shrubland, mainly due to the canopy coverage caused by habitat differences [37]. This difference indicates the necessity of distinguishing vegetation biomes in the study of *NPP* dynamics in desert steppe ecosystems.

Spatially, the annual average of *NPP* in the south was greater than 200 g C m^{-2} y^{-1}, and generally higher than the value in the north by about 100 g C m^{-2} y^{-1}. The spatial distribution of *NPP* in the desert steppe was similar to the precipitation contour, which shows the importance of climatic variables in the spatial distribution of *NPP*. The study area is affected by the East Asian monsoon climate, and the distribution of precipitation decreases from south to north and west. Therefore, the spatial distribution of *NPP* may be dominated by climatic factors in the desert steppe.

4.2. NPP Dynamics and Main Driving Processes

The poor habitability of the study area provides an independent observation platform with a relatively specific environmental disturbance factor for this study. The average annual change rate of *NPP* was 1.13 g C m^{-2} y^{-1}, with an insignificant increase. However, there was a significant increase in only 5.5% of our study area. This phenomenon mainly appears in the western and northern parts of the study area, and the *NPP* was usually less than 150 g C m^{-2} y^{-1}. Therefore, the regions with relatively low *NPP* in the desert steppe showed a more obvious vulnerability to climate change.

Our study found that the regions with significant changes in *NPP* generally had lower precipitation in the desert steppe. This result is consistent with the results of the correlation analysis between *NPP* and precipitation in the temporal dimension, showing that precipitation was an important driving factor for *NPP* changes in arid and semi-arid ecosystems. In terms of time-scale comparison, the effects of precipitation changes in the desert steppe's productivity in the growing season and on the annual scale were consistent. The impact of precipitation changes outside of the growing season on *NPP* was not significant in grass- nor shrub-dominated biomes. In contrast, previous studies have shown that precipitation outside of the growing season is significantly beneficial to the carbon sequestration of grassland biomes, and that it causes carbon biomass to increase [38]. However, neither the *NPP* changes of the grassland biome nor the shrub-dominated biome showed a significant response to precipitation outside of the growing season in our study. This may be due to the fact that precipitation outside the growing season has a more significant effect on the underground part of the vegetation in the desert steppe. Precipitation changes significantly affect soil microbial community structure, quality and activity in arid regions, which in turn interfere with root growth and exudates of grasses to limit total plant biomass [39,40]. However, this phenomenon cannot be estimated at the regional scale by the photosynthetically active radiation model (CASA) based on satellite observations. Therefore, the effects of precipitation outside the growing season on the desert steppe's productivity and carbon cycle need to be further verified by reasonable field experiments.

Temperature is an important limiting factor of productivity dynamics in mid-latitude steppe ecosystems in the Northern Hemisphere [41,42]. Our study shows that there was a negative correlation between temperature and *NPP* in both grass- and shrub-dominated biomes during the growing season. The effects of annual and outside-of-growing-season temperature changes were not significantly different between the two biomes. However, in the spatial dimension, the area where the temperature was significantly correlated with *NPP* accounted for 12% (average *NPP* was 144.6 g C m^{-2} y^{-1}) on the annual scale and 43% (average *NPP* was 139.8 g C m^{-2} y^{-1}) during the growing season. The average *NPP* of the remaining 31% of the region was 148.1 g C m^{-2} y^{-1}, which was significantly negatively correlated during the growing season but not on the annual scale. This suggests that the higher the productivity of desert steppe vegetation, the stronger the stress resistance and resilience to large temperature changes during the growing season. This may be due to the fact that vegetation with higher productivity usually has a more developed root system, which in turn imparts stronger nutrient uptake and transport capabilities [43]. This will help the vegetation maintain normal physiological and metabolic activities under extreme temperature events. Therefore, vegetation with higher productivity in the desert steppe has better resistance and resilience to temperature changes during the growing season.

4.3. Uncertainties and Limitations

Light-use-efficiency models have been widely used to estimate the net primary productivity of regional vegetation. To perform regional-scale simulations, we applied kriging interpolation to scale the site data to the pixel level. The more stations there are in the interpolation process, the less uncertainty in the results [44]. There were six national standard weather stations in the study area, as well as other extra-regional weather stations in the east, south, and west. In future research, meteorological data from outside of China to the north will be supplemented, which will improve the accuracy of our data expansion. In addition, the towns in the study area are few and concentrated, and the local government has implemented extensive policies related to steppe enclosure management and controlling grazing intensity. However, grazing is still one of the most important factors affecting the accuracy of *NPP* estimation. Therefore, in order to accurately simulate the driving mechanisms of *NPP*, we need to improve the constraints of the above conditions in future work.

5. Conclusions

The annual average *NPP* of the desert steppe in Inner Mongolia was 131.93 g C m^{-2} y^{-1}, and the average *NPP*s of the grass- and shrub-dominated biomes were 141.8 and 90.6 g C m^{-2} y^{-1}, respectively. The *NPP* increased faster in the grassland biome than in the shrub-dominated biome. Precipitation and temperature at different time scales showed a slow upward trend, and the degree of aridity tended to weaken. Precipitation and temperature changes have significant effects on desert steppe *NPP*, with precipitation changes being the dominant factor. As for our hypothesis, the results indicate that the grass- and shrub-dominated biomes did not show significant differences due to changes in climatic variables. However, we found that when the net primary productivity of the desert steppe vegetation was greater than 150 g C m^{-2} y^{-1}, it was beneficial to the vegetation's resistance and resilience to high temperature during the growing season. We conclude that, if vegetation maintains high productivity levels and the area adheres to controlled grazing intensity, the vegetation will be better able to adapt to frequent high-temperature and drought events in the mid-latitude region, and the sustainable development of the steppe ecosystem will be maintained.

Author Contributions: B.Y.: conceptualization and writing of the draft; X.L.: methodology, writing and editing; Y.X.: formal analysis and software; Y.C.: funding acquisition, project administration, and supervision; M.L.: visualization. K.Y.: data curation; X.Q.: software. All authors have read and agreed to the published version of the manuscript.

Funding: This research was supported by the 2021 Young Teachers' Scientific Research Ability Improvement Plan of Northwest Normal University, and the Innovation Fund for Colleges and Universities of the Department of Education, Gansu Province, China (grant no. 2021B-079).

Acknowledgments: We thank the anonymous reviewers for their comments.

Conflicts of Interest: The authors declare no conflict of interest.

References

1. Sun, H.; Chen, Y.; Xiong, J.; Ye, C.; Yong, Z.; Wang, Y.; He, D.; Xu, S. Relationships between climate change, phenology, edaphic factors, and net primary productivity across the Tibetan Plateau. *Int. J. Appl. Earth Obs. Geoinf.* **2022**, *107*, 102708. [CrossRef]
2. Mayer, A.; Kaufmann, L.; Kalt, G.; Matej, S.; Theurl, M.C.; Morais, T.G.; Leip, A.; Erb, K.-H. Applying the Human Appropriation of Net Primary Production framework to map provisioning ecosystem services and their relation to ecosystem functioning across the European Union. *Ecosyst. Serv.* **2021**, *51*, 101344. [CrossRef] [PubMed]
3. Bengtsson, J.; Bullock, J.; Egoh, B.; Everson, C.; Everson, T.; O'Connor, T.; O'Farrell, P.; Smith, H.; Lindborg, R. Grasslands—More important for ecosystem services than you might think. *Ecosphere* **2019**, *10*, e02582. [CrossRef]

4. Peng, F.; Xue, X.; You, Q.; Huang, C.; Dong, S.; Liao, J.; Duan, H.; Tsunekawa, A.; Wang, T. Changes of soil properties regulate the soil organic carbon loss with grassland degradation on the Qinghai-Tibet Plateau. *Ecol. Indic.* **2018**, *93*, 572–580. [CrossRef]
5. Li, J.; Chen, H.; Zhang, C. Impacts of climate change on key soil ecosystem services and interactions in Central Asia. *Ecol. Indic.* **2020**, *116*, 106490. [CrossRef]
6. Li, D.; Wu, S.; Liu, L.; Zhang, Y.; Li, S. Vulnerability of the global terrestrial ecosystems to climate change. *Glob. Change Biol.* **2018**, *24*, 4095–4106. [CrossRef]
7. Zhang, C.; Zhang, Y.; Wang, Z.; Li, J.; Odeh, I. Monitoring phenology in the temperate grasslands of China from 1982 to 2015 and its relation to net primary productivity. *Sustainability* **2019**, *12*, 12. [CrossRef]
8. Gao, Q.; Zhu, W.; Schwartz, M.W.; Ganjurjav, H.; Wan, Y.; Qin, X.; Ma, X.; Williamson, M.A.; Li, Y. Climatic change controls productivity variation in global grasslands. *Sci. Rep.* **2016**, *6*, 26958. [CrossRef]
9. Liu, Y.; Zhou, R.; Wen, Z.; Khalifa, M.; Zheng, C.; Ren, H.; Zhang, Z.; Wang, Z. Assessing the impacts of drought on net primary productivity of global land biomes in different climate zones. *Ecol. Indic.* **2021**, *130*, 108146. [CrossRef]
10. Sha, Y.; Shi, Z.; Liu, X.; An, Z. Distinct impacts of the Mongolian and Tibetan Plateaus on the evolution of the East Asian monsoon. *J. Geophys. Res. Atmos.* **2015**, *120*, 4764–4782. [CrossRef]
11. Shi, Z.; Liu, X.; Liu, Y.; Sha, Y.; Xu, T. Impact of Mongolian Plateau versus Tibetan Plateau on the westerly jet over North Pacific Ocean. *Clim. Dyn.* **2015**, *44*, 3067–3076. [CrossRef]
12. Liu, Y.Y.; Evans, J.P.; McCabe, M.F.; De Jeu, R.A.; van Dijk, A.I.; Dolman, A.J.; Saizen, I. Changing climate and overgrazing are decimating Mongolian steppes. *PLoS ONE* **2013**, *8*, e57599.
13. John, R.; Chen, J.; Kim, Y.; Ouyang, Z.; Xiao, J.; Park, H.; Shao, C.; Zhang, Y.; Amarjargal, A.; Batkhshig, O. Differentiating anthropogenic modification and precipitation-driven change on vegetation productivity on the Mongolian Plateau. *Landsc. Ecol.* **2016**, *31*, 547–566. [CrossRef]
14. Liu, X.; Ma, Q.; Yu, H.; Li, Y.; Li, L.; Qi, M.; Wu, W.; Zhang, F.; Wang, Y.; Zhou, G. Climate warming-induced drought constrains vegetation productivity by weakening the temporal stability of the plant community in an arid grassland ecosystem. *Agric. For. Meteorol.* **2021**, *307*, 108526. [CrossRef]
15. Hou, E.; Litvak, M.E.; Rudgers, J.A.; Jiang, L.; Collins, S.L.; Pockman, W.T.; Hui, D.; Niu, S.; Luo, Y. Divergent responses of primary production to increasing precipitation variability in global drylands. *Glob. Chang. Biol.* **2021**, *27*, 5225–5237. [CrossRef] [PubMed]
16. Ravi, S.; Law, D.J.; Caplan, J.S.; Barron-Gafford, G.A.; Dontsova, K.M.; Espeleta, J.F.; Villegas, J.C.; Okin, G.S.; Breshears, D.D.; Huxman, T.E. Biological invasions and climate change amplify each other's effects on dryland degradation. *Glob. Chang. Biol.* **2022**, *28*, 285–295. [CrossRef]
17. Guo, L.; Li, J.; He, W.; Liu, L.; Huang, D.; Wang, K. High nutrient uptake efficiency and high water use efficiency facilitate the spread of Stellera chamaejasme L. in degraded grasslands. *BMC Ecol.* **2019**, *19*, 50. [CrossRef]
18. Knapp, A.K.; Briggs, J.M.; Collins, S.L.; Archer, S.R.; Bret-Harte, M.S.; Ewers, B.E.; Peters, D.P.; Young, D.R.; Shaver, G.R.; Pendall, E. Shrub encroachment in North American grasslands: Shifts in growth form dominance rapidly alters control of ecosystem carbon inputs. *Glob. Chang. Biol.* **2008**, *14*, 615–623. [CrossRef]
19. Zhu, W.; Pan, Y.; He, H.; Yu, D.; Hu, H. Simulation of maximum light use efficiency for some typical vegetation types in China. *Chin. Sci. Bull.* **2006**, *51*, 457–463. [CrossRef]
20. Field, C.B.; Randerson, J.T.; Malmström, C.M. Global net primary production: Combining ecology and remote sensing. *Remote Sens. Environ.* **1995**, *51*, 74–88. [CrossRef]
21. Wang, Y.; Xu, X.; Huang, L.; Yang, G.; Fan, L.; Wei, P.; Chen, G. An improved CASA model for estimating winter wheat yield from remote sensing images. *Remote Sens.* **2019**, *11*, 1088. [CrossRef]
22. Potter, C.S.; Randerson, J.T.; Field, C.B.; Matson, P.A.; Vitousek, P.M.; Mooney, H.A.; Klooster, S.A. Terrestrial ecosystem production: A process model based on global satellite and surface data. *Glob. Biogeochem. Cycles* **1993**, *7*, 811–841. [CrossRef]
23. Zhu, W.; Pan, Y.; He, H.; Wang, L.; Mou, M.; Liu, J. A changing-weight filter method for reconstructing a high-quality NDVI time series to preserve the integrity of vegetation phenology. *IEEE Trans. Geosci. Remote Sens.* **2011**, *50*, 1085–1094. [CrossRef]
24. Li, G.; Li, X.; Zhou, T.; Wang, H.; Li, R.; Wang, H.; Wei, D. A model for simulating the soil organic carbon pool of steppe ecosystems. *Environ. Modeling Assess.* **2016**, *21*, 339–355.
25. Zhang, G.; Zhou, G.; Chen, F.; Wang, Y. Analysis of the variability of canopy resistance over a desert steppe site in Inner Mongolia, China. *Adv. Atmos. Sci.* **2014**, *31*, 681–692. [CrossRef]
26. Yang, F.; Zhou, G. Characteristics and modeling of evapotranspiration over a temperate desert steppe in Inner Mongolia, China. *J. Hydrol.* **2011**, *396*, 139–147. [CrossRef]
27. Ruimy, A.; Saugier, B.; Dedieu, G. Methodology for the estimation of terrestrial net primary production from remotely sensed data. *J. Geophys. Res. Atmos.* **1994**, *99*, 5263–5283. [CrossRef]
28. Tong, S.; Lai, Q.; Zhang, J.; Bao, Y.; Lusi, A.; Ma, Q.; Li, X.; Zhang, F. Spatiotemporal drought variability on the Mongolian Plateau from 1980–2014 based on the SPEI-PM, intensity analysis and Hurst exponent. *Sci. Total Environ.* **2018**, *615*, 1557–1565. [CrossRef]
29. Beguería, S.; Vicente-Serrano, S.M.; Angulo-Martínez, M. A multiscalar global drought dataset: The SPEIbase: A new gridded product for the analysis of drought variability and impacts. *Bull. Am. Meteorol. Soc.* **2010**, *91*, 1351–1356. [CrossRef]
30. Tirivarombo, S.; Osupile, D.; Eliasson, P. Drought monitoring and analysis: Standardised precipitation evapotranspiration index (SPEI) and standardised precipitation index (SPI). *Phys. Chem. Earth Parts A/B/C* **2018**, *106*, 1–10. [CrossRef]

31. Zhou, J.; Jia, L.; Menenti, M. Reconstruction of global MODIS NDVI time series: Performance of harmonic analysis of time series (HANTS). *Remote Sens. Environ.* **2015**, *163*, 217–228. [CrossRef]
32. Zhang, X.; Sun, S.; Yong, S.; Zhou, Z.; Wang, R. *Vegetation Map of the People's Republic of China (1: 1000000)*; Geology Publishing House: Beijing, China, 2007.
33. Zhu, E.; Pan, Y.; Zhang, J. Remote sensing estimation of net primary productivity of terrestrial vegetation in China. *J. Plant Ecol.* **2007**, *31*, 413–424. (In Chinese)
34. Huang, Q.; Zhang, F.; Zhang, Q.; Ou, H.; Jin, Y. Quantitative assessment of the impact of human activities on terrestrial net primary productivity in the Yangtze River delta. *Sustainability* **2020**, *12*, 1697. [CrossRef]
35. Zhu, Q.; Zhao, J.; Zhu, Z.; Zhang, H.; Zhang, Z.; Guo, X.; Bi, Y.; Sun, L. Remotely sensed estimation of net primary productivity (NPP) and its spatial and temporal variations in the Greater Khingan Mountain region, China. *Sustainability* **2017**, *9*, 1213. [CrossRef]
36. Hossain, M.L.; Kabir, M.H.; Nila, M.U.S.; Rubaiyat, A. Response of grassland net primary productivity to dry and wet climatic events in four grassland types in Inner Mongolia. *Plant-Environ. Interact.* **2021**, *2*, 250–262. [CrossRef]
37. Han, Z.; Song, W.; Deng, X.; Xu, X. Grassland ecosystem responses to climate change and human activities within the Three-River Headwaters region of China. *Sci. Rep.* **2018**, *8*, 9079. [CrossRef] [PubMed]
38. Yang, B.; Gong, J.; Zhang, Z.; Wang, B.; Zhu, C.; Shi, J.; Liu, M.; Liu, Y.; Li, X. Stabilization of carbon sequestration in a Chinese desert steppe benefits from increased temperatures and from precipitation outside the growing season. *Sci. Total Environ.* **2019**, *691*, 263–277. [CrossRef]
39. Bi, B.; Wang, K.; Zhang, H.; Wang, Y.; Fei, H.; Pan, R.; Han, F. Plants use rhizosphere metabolites to regulate soil microbial diversity. *Land Degrad. Dev.* **2021**, *32*, 5267–5280. [CrossRef]
40. Li, Z.; Wang, F.; Su, F.; Wang, P.; Li, S.; Bai, T.; Wei, Y.; Liu, M.; Chen, D.; Zhu, W. Climate change drivers alter root controls over litter decomposition in a semi-arid grassland. *Soil Biol. Biochem.* **2021**, *158*, 108278. [CrossRef]
41. Huang, Q.; Ju, W.; Zhang, F.; Zhang, Q. Roles of climate change and increasing CO_2 in driving changes of net primary productivity in China simulated using a dynamic global vegetation model. *Sustainability* **2019**, *11*, 4176. [CrossRef]
42. Yu, L.; Gu, F.; Huang, M.; Tao, B.; Hao, M.; Wang, Z. Impacts of 1.5 °C and 2 °C global warming on net primary productivity and carbon balance in China's terrestrial ecosystems. *Sustainability* **2020**, *12*, 2849. [CrossRef]
43. Liu, M.; Gong, J.; Li, Y.; Li, X.; Yang, B.; Zhang, Z.; Yang, L.; Hou, X. Growth-defense trade-off regulated by hormones in grass plants growing under different grazing intensities. *Physiol. Plant.* **2019**, *166*, 553–569. [CrossRef] [PubMed]
44. Pellicone, G.; Caloiero, T.; Modica, G.; Guagliardi, I. Application of several spatial interpolation techniques to monthly rainfall data in the Calabria region (southern Italy). *Int. J. Climatol.* **2018**, *38*, 3651–3666. [CrossRef]